2014 Health Innovations and Point-of-Care Technologies Conference
Seattle, Washington USA, October 8-10, 2014

DNA Ploidy Measure of Feulgen-Stained Cancer Cells using Three-Dimensional Image Cytometry

Nitin Agarwal-*IEEE* Member, Yiting Xie-*IEEE Member*, Florence W. Patten, Anthony P. Reeves-*Senior IEEE Member*, and Eric J. Seibel-*Senior IEEE Member*

***Abstract*— The clinical utility of DNA ploidy as prognostic indicator is well established for cancer. Quantitative measures of DNA are possible in cell populations with flow cytometry (FCM) and individual cells with image cytometry (ICM). Because ICM can be more accurate in 3D images of absorptive stained DNA, we studied a new 3D optical microscope, the Cell-CT™. By providing quantitative cytometry of cells moving in a microcapillary tube with 3D visualization of morphology, the Cell-CT combines attributes of both FCM and ICM. Comparing Cell-CT to standard FCM, DNA ploidy measurements of Feulgen stained cultured cancer cells were made using fully automated 3D nuclear segmentation. There was a significant Spearman's rank correlation ($r=0.98$, $p<0.01$) between the results from FCM and Cell-CT, while determining nuclear morphology of seven different cell types. We conclude that Cell-CT provides measurements of DNA content comparable to FCM and is a valuable alternative method for assessing tumorgenesis of enriched microsamples of diagnostic cells.**

I. Introduction

Diagnostic and prognostic utility of quantitative DNA ploidy has been demonstrated for selected solid malignant neoplasms like bladder, breast, colon, lung, endometrium, ovary, prostate and melanoma [1-4]. It has been confirmed that chromosomal aneuploidy is an early key event in tumorgenesis caused by genetic instability [5]. Flow cytometry (FCM), a standard technique for DNA ploidy has high throughput but lacks visual distinction between individual cancer cells and normal cells. Further it needs a large sample size (>10,000 cells) and cannot distinguish aneuploidy in single cells in spite of measuring DNA content per cell, because the measurement in FCM is a distribution of DNA content (histogram) for the entire population of cells. Thus microsample of cells from tumors can be masked by the presence of non-tumor, inflammatory or normal diploid population [6-8].

Image cytometry (ICM) using Feulgen staining is an alternative technique to FCM for detection of DNA ploidy [6, 4]. ICM has advantages as the set-up cost is low, a small number of nuclei are required, and visual morphological distinction between a cancer cell and a normal cell, (an important attribute for cytopathologists) is provided [6, 7]. Since individual cells are analyzed, ICM can identify occasional abnormal cells in the sample. However, ICM uses only two-dimensional (2D) images for analysis, whereas the morphology of cells and their nuclear chromatin features are all three-dimensional (3D). Challenges in quantification are from the difficulty in segmenting morphological features in 2D ICM images and extrapolating to 3D volumes. Hence, DNA ploidy measures from conventional ICM are not highly accurate prognostic indicators of cancer state and its progression.

Recently, techniques for obtaining 3D information about biological samples have been developed [9-11]. However, all are limited to either analyzing tissue samples or analyzing confocal images using fluorescent dyes, making it unsuitable for current needs of cytopathologists who rely on absorption based stains [12]. Absorption measurement is the corner stone of clinical cytopathology and thus there has been a need for isotropic, high-resolution, quantitative 3D imaging using absorption staining. Although cytopathologists have a foundation of knowledge with absorption stains, future inclusion of fluorescence imaging using probed biomarkers could further assist in early disease diagnosis and rapid treatment selection.

In this study a Cell-CT™ (VisionGate Inc. Phoenix, AZ) was used which is an optical projection tomographic microscope co-developed at the University of Washington Seattle [13, 14]. The choice of Feulgen staining method and automated 3D nuclear segmentation technique to compute the DNA ploidy of seven cultured cancer cells as an alternative to traditional two-dimensional ICM was based on a previous study [15]. Cell-CT provides 3D, submicron, isometric and high-resolution images of cellular nuclear features [15]. Since the entire volume of the nucleus is measured, there can be less uncertainty in the measurement of total DNA content. In addition, Cell-CT performs multimodal imaging generating both bright field transmission image as well as a fluorescence image with exact co-registration [15]. The Cell-CT combines attributes of computed tomography (CT) imaging with slow-flow cytometry. Thus, it provides quantitative cytometry along with 3D visualization of morphology. DNA ploidy analysis results from Cell-CT were later compared for accuracy with the FCM. Morphology was also visually confirmed for all cancer cells with assistance from an experienced cytopathologist.

II. Methods

A. Samples for comparative study of ICM and FCM

A total of seven cultured human cancer lines consisting of

Funding for this interdisciplinary & collaborative NSF project was provided by National Science Foundation grant # CBET-1014976 & 1014813 (PI's are E.J Seibel & A.P. Reeves).

N. Agarwal graduated from the Dept. of Bioengineering, University of Washington, Seattle, WA 98195 USA. He is now working with VisionGate Inc., Phoenix, AZ 85034 USA. (Corresponding author to provide phone: 404-919-3292; fax: 206-685-8047; e-mail: agarwaln@uw.edu).

Y. Xie and A.P Reeves are with School of Electrical and Computer Engineering, Cornell University, Ithaca NY 77005 USA. (e-mail: yx269@cornell.edu, reeves@ece.cornell.edu).

F.W. Patten is a cytopathologist who retired last year from VisionGate Inc. (e-mail: fwpcfiac@earthlink.net).

E. J. Seibel is with the Dept. of Mechanical Engineering, University of Washington, Seattle, WA 98195 USA. (e-mail: eseibel@uw.edu).

A549 (lung adenocarcinoma), BT-474 (breast carcinoma), Caco-2 (colorectal adenocarcinoma), Hep G2 (liver carcinoma), HT-29 (colorectal adenocarcinoma), PC3 (prostate carcinoma) and SK-BR-3 (breast adenocarcinoma) cells from ATCC® were used. Trout erythrocyte nuclei (TEN) (Biosure, Inc. USA) and human lymphocytes (HemaCare Corporation, USA) were used as internal reference standards to determine the position of the diploid peak (2c) on Cell-CT and FCM respectively (Fig. 5).

B. Flow Cytometry

Standard FCM was performed on all the cancer cells and lymphocytes, which were fixed in 50% ethanol according to the conventional protocol and the manufacturer's instruction [16]. Each sample was resuspended in an isotonic pH 7.4-buffered solution with 0.1% nonidet P-40 detergent, 10 µg/ml diamidino-2-phenylindole (DAPI) and 1% RNAse, triturated with a 26 gauge needle, and filtered through 40 µm steel mesh. The analysis was performed using an InFlux cytometer (BD Biosciences, USA) with UV excitation. A total of 20,000 cells were analyzed, and in all cases, a coefficient of variation (CV) of below 5.0% was found. The DNA index and S-phase fraction (SPF) were analyzed for each cancer cell in comparison with lymphocytes using the software program MultiCycle [17] (Phoenix Flow Systems, San Diego, CA, USA).

C. Image Cytometry

Image Acquisition: The setup used for this experiment consisted of Cell-CT, a 546±20 nm green filter, a monochromatic CCD camera (Prosilica GE1650, Allied Vision Technologies, Germany). Cell-CT was built using a wide field optical microscope (Olympus IX71) and a custom-designed microcapillary base rotation stage [13-15]. Each cultured cancer cell along with TEN was stained using standard Feulgen staining technique [15, 18]. The stained cells were mixed with an optical gel (Nye SmartGel OC431A- LVP) and flowed through a 50-micron inner diameter capillary tube. The tube rotates in an oil-filled space between two flat, parallel glass slides. These parallel glass slides are later inserted into the Cell-CT for acquisition of 3D cellular images [15]. A pseudo-projection image was taken by axially scanning the objective focal plane through the sample and optically integrating all the focal plane images. 500 such pseudo-projection images were taken in one rotation at uniform angular intervals of 0.72 degrees. The 3D structure of the specimen was then obtained by reconstructing these 500 2D pseudo-projections using filtered backprojection algorithms, similar to X-ray CT [19].

DNA Ploidy Analysis: Fully automated 3D segmentation for nucleus and cytoplasmic regions on Cell-CT images was performed using graph cut [20] with convex hull algorithm [21] at Cornell University.

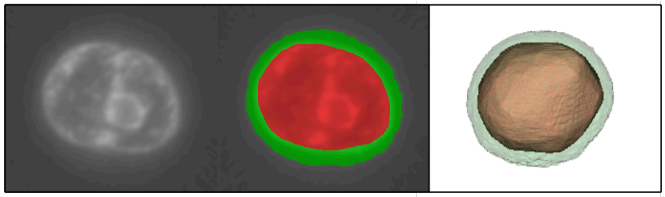

Figure 1. Graph cut with convex hull algorithm. From left to right: central slice of a BT-474 cancer cell, segmentation using graph-cut with convex hull and its 3D visualization. Red region denotes the segmented nucleus and green region denotes the segmented cytoplasm.

Graph cut formulates segmentation as a binary problem: a pixel is either labeled as an object or background. The following steps were used: (1) Graph-cut algorithm was applied to an intensity normalized 3D cell image (Fig. 1). The segmented 'object' was considered the nucleus and the 'background' was the cytoplasm plus the outside cell background. (2) In order to better segment the cancer cells with intensity variations within the nucleus, a 3D convex hull algorithm was used on the segmented nucleus to ensure that it was a connected convex region. (3) Intensity values in the segmented nucleus region were set lower so that they were similar to the intensities in adjacent cytoplasm regions; then graph-cut algorithm was reapplied. The segmented 'object' was now considered as the entire cell. The cytoplasm was obtained by subtracting the nucleus part from the cell.

Using the above segmentation algorithm, 3D segmentation of one hundred A549, BT-474, Caco-2, HT-29, Hep G2, PC3 and SK-BR-3 cells were achieved (along with their respective TENs). Camera sensor was assumed to be linear and uniform filtered illumination was maintained. All samples were fixed, stained, and imaged under constant conditions, to allow a direct comparison of the measured data. Optical density and nuclear area were measured and integrated optical density (IOD) of each cancer cell nucleus was calculated. Similarly IOD of the corresponding TEN's was calculated and scaled to match the IOD of normal human diploid cell. These were then used as reference cells to determine the position of the normal diploid peak (2c). A histogram of DNA content was produced for each cancer cell and ploidy related parameters such as DNA index (DI) and percentage of cells exceeding 5c were calculated [5].

Histograms were analyzed according to European Society for Analytical Cellular Pathology guidelines (ESACP) [18]. Specimen was defined as:

- Diploid: When there was only one peak (which was 2c, or DI = 0.9–1.1) during the G0 or G1 phase, when the number of 4c nuclei during the peak of the G2 phase did not exceed 6% of the total, or when the number of nuclei with a DNA content of >5c did not exceed 1% of the total.
- Tetraploid: When there was a population of 4c nuclei (DI = 1.9–2.1) >6% of the total, representing stage G2 of the cell cycle. It means DNA content is indistinguishable from that of tetraploid cells, with a percentage of these cells disproportionately higher than that of the S phase fraction.
- Aneuploid: When there was a population of nuclei with abnormal DNA content, separated from the diploid peak (DI > 1.1), and representing >2.5% of the total or when the number of nuclei with a DNA content of >5c or 9c exceeded 1% of the total.

D. Statistical Methods

All analysis was performed using Microsoft Excel and MATLAB (MathWorks, Version R2012a, Natick, MA,

USA). Regression analysis with estimation of Spearman's rank coefficient was used to compare the DNA indices from FCM and Cell-CT.

III. Results

Table 1 lists the DNA indices and DNA ploidy analysis according to ESACP [18]. There was a significant Spearman's rank correlation ($r=0.98$, $p<0.01$) between the results from FCM and Cell-CT (Fig. 2). Good concordance was also achieved between histograms of FCM and Cell-CT for all cancer cell lines tested (e.g. Fig. 5 shows results for SK-BR-3 cell line).

Table 1. Comparison of DNA ploidy analysis from FCM and Cell-CT.

Specimen	DNA index by Cell-CT	DNA Ploidy by Cell-CT	DNA Index by FCM	DNA Ploidy by FCM
Hep G2	1.66	Aneuploid	1.52	Aneuploid
A549	1.83	Aneuploid	1.76	Aneuploid
PC3	2.01	Tetraploid	2.09	Tetraploid
HT-29	2.14	Aneuploid	2.03	Aneuploid
Caco-2	2.44	Aneuploid	2.41	Aneuploid
SK-BR-3	2.47	Aneuploid	2.27	Aneuploid
BT-474	3.33	Aneuploid	3.22	Aneuploid

Further, we successfully preserved the nuclear morphology of all cancer cells and TEN's. Fig. 3 compares the nuclear morphology of a typical human lung adenocarcinoma with a TEN. All cancer cell lines showed heterogeneous chromatin content (Fig. 4), a typical characteristic of cancer cells.

IV. Discussion

We have combined some benefits of FCM and traditional 2D ICM by developing a technique, which can analyze the DNA content of individual cells in 3D without compromising its nuclear morphology. Using a population of 100 cells, we showed good correlation between DNA indices from Cell-CT with automated 3D segmentation, and FCM using 20,000 cells from the same seven cancer cell lines.

Unlike FCM or ICM, Cell-CT provides 3D morphometric data like volume, shape and nuclear texture, which is very important for cytopathologists who primarily rely on cellular morphology for cancer diagnosis. We showed clear visualization of heterogeneous chromatin content of A549 cells along with tubular invaginations originating from nuclear membrane projecting inwards, a prominent characteristic in some cancer cells (Fig. 3) [22, 23].

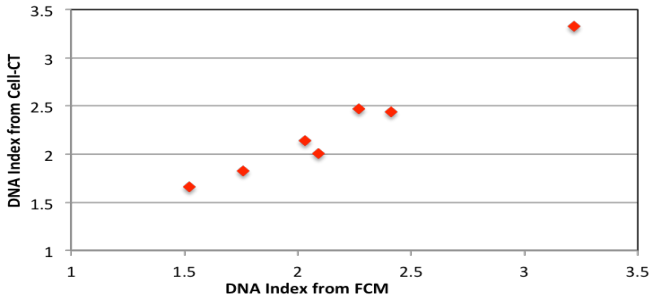

Figure 2. Comparison of DNA indices: There is a high correlation $r=0.98$, $p<0.01$) between the DNA indices from FCM and Cell-CT.

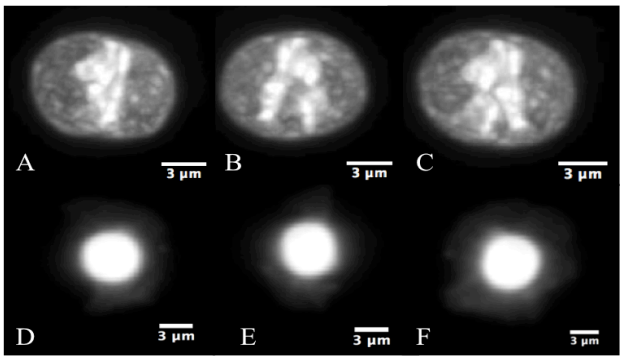

Figure 3. Comparison of images of (A): Axial, (B): Sagittal and (C): Coronal views of A549 cell (human lung adenocarcinoma) with images of (D): Axial, (E): Sagittal and (F): Coronal views of TEN (trout erythrocyte nuclei).

To our knowledge this is the first validation study that has quantitatively measured DNA content in 3D using absorption stains. Previous studies with FCM, though had shown correlation of 0.96, were restricted to 2D nuclear images [6, 24, 25]. We have not only shown improved correlation but also preserved nuclear morphology through 3D imaging.

A major advantage of Cell-CT is that it acquires single cell images with equal resolution in all directions for accurate 3D image analysis. This makes automated 3D segmentation robust for rare, single cell analysis without having any complications of fragmentation and overlapping of cells. However, the acquisition of 3D images is currently at very low throughput. Engineering higher throughput with improved image quality is an ongoing challenge [26]. Though there are techniques, which perform high throughput image cytometry like ImageStream [27] and STEAM flow analyzer [28], they only analyze cells in a single perspective.

The Cell-CT has recently been shown to make semi-automated diagnosis of lung cancer highly accurate in small population of cells like sputum specimens [29]. By enriching lung epithelial cells, a more accurate but slower diagnostic system of 3D-image based morphology and DNA index cytometry can be a cost-effective red-flagging triage for subsequent X-ray CT-scanning follow-up of high risk patients.

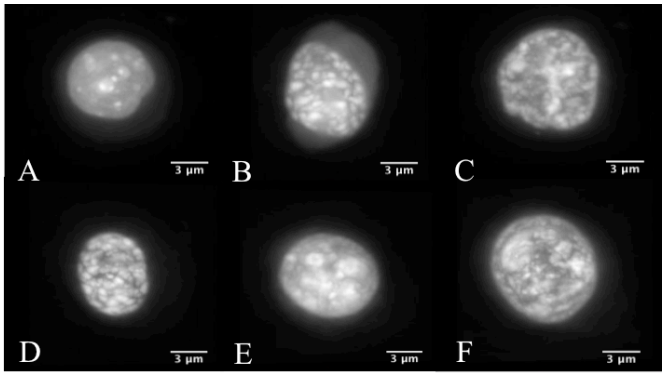

Figure 4. Representative Cell-CT axial images of (A). Caco-2 cell (human colorectal adenocarcinoma), (B). Hep G2 cell (human liver carcinoma), (C). HT-29 cell (human colorectal adenocarcinoma), (D). PC3 cell (human prostate carcinoma), (E). SK-BR-3 cell (human breast adenocarcinoma) and (F). BT-474 cell (human breast carcinoma) stained with Feulgen technique. The images show dense nuclear DNA staining along with light residual cytoplasmic staining.

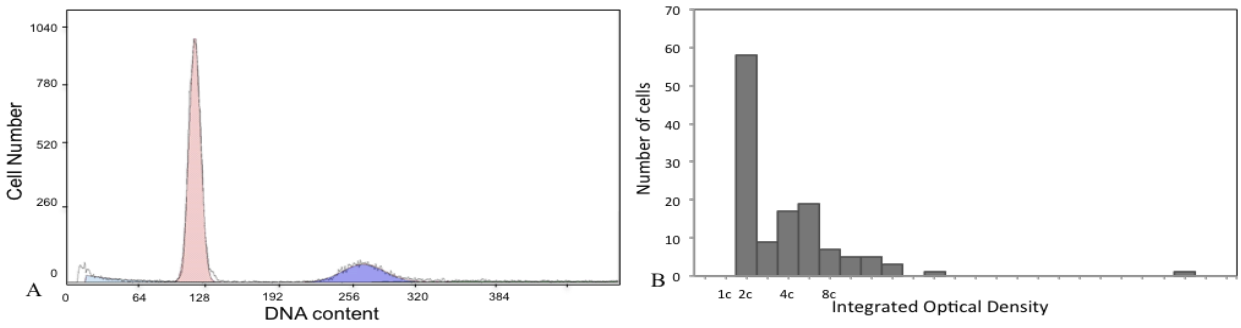

Figure 5. Histograms showing DNA distribution of SK-BR-3 by flow cytometry and Cell-CT (from left to right). The FCM has two peaks; the pink at 122 channel represents the normal diploid population (2c) of lymphocytes while the smaller blue peak at 277 channel represents aneuploidy population (>2c) of SK-BR-3 making the DNA index 2.27. The Cell-CT shows good concordance (defined by ESACP) having a prominent diploid peak (2c) of scaled TENs with a small aneuploid peak (>2c) of SK-BR-3 making the DI 2.47.

V. Conclusion And Future Work

We conclude that FCM and Cell-CT provide comparable measurements of DNA content though further validation with clinical cancer specimens is required. Cell-CT provides a valuable alternative method for assessing tumorgenesis and may offer certain advantages over FCM when only microsample sizes are available.

Acknowledgment

The authors thank Yuriana Garcia for assisting in data collection, Donna Prunkard and Dr. Peter Rabinovitch of Dept. of Pathology at University Washington Seattle for helping with staining and flow cytometry.

References

[1] D. E. Merkel, L. G. Dressler and W. L. McGuire, Flow cytometry, cellular DNA content, and prognosis in human malignancy, *J. Clin. Oncol*., vol. 5, pp. 1690–1703, 1987.

[2] H. Joensuu, S. Toikkanen and P. J. Klemi, DNA index & S-phase fraction & their combination as prognostic factors in operable ductal breast carcinoma, *Cancer*, vol. 66, pp. 331–340, 1990.

[3] A. E. Reles, C. Gee, I. Schellschmidt et al., Prognostic significance of DNA content & S-phase fraction in epithelial ovarian carcinomas analyzed by image cytometry, *Gynecol. Oncol.*, vol. 71, pp. 3–13, 1998.

[4] J. M. Dunn, G. D. Mackenzie, D. Oukrif et al., Image cytometry accurately detects DNA ploidy abnormalities & predicts late relapse to high-grade dysplasia and adenocarcinoma in Barrett's oesophagus following photodynamic therapy, *Br. J. Cancer,* vol. 102, pp. 1608–1617, 2010.

[5] G. Haroske, J. P. Baak, H. Danielsen et al., Fourth updated ESACP consensus report on diagnostic DNA image cytometry, *Anal Cell Pathol.,* vol. 23, pp. 89–95, 2001.

[6] D. A. Ellison, S. J. Maygarden and D. B. Novotny, Quantitative DNA analysis of fresh solid tumors by flow & image cytometric methods: a comparison using the Roche Pathology Workstation Image Analyzer, *Mod. Pathol.,* vol. 8, pp. 275–281, 1985.

[7] A. Pindur, S. Chakraborty, D. G. Welch et al., DNA ploidy measurements in prostate cancer: Differences between image analysis & flow cytometry and clinical implications, *Prostate,* vol. 25, pp. 189–198, 1994.

[8] K. A. Alanen, M. Lintu and H. Joensuu, Image cytometry of breast carcinomas that are DNA diploid by flow cytometry: time to revise the concept of DNA diploidy?, *Anal. Quant. Cytol. Histol*., vol. 20(3), pp. 178-186, 1998.

[9] J. Sharpe, Optical Projection Tomography as a Tool for 3D Microsco--py & Gene Expression Studies, *Science*, vol. 296, pp. 541–545, 2002.

[10] T. Alanentalo, A. Asayesh, H. Morrison et al., Tomographic molecular imaging & 3D quantification within adult mouse organs, *Nat Meth*, vol. 4, pp. 31–33, 2007.

[11] F. Pampaloni, E. G. Reynaud and E.K. Stelzer, The third dimension bridges the gap between cell culture & live tissue, *Nat. Rev. Mol. Cell Biol.,* vol. 8, pp. 839–845, 2007.

[12] Y. Garini, B. J. Vermolen and I. T. Young, From micro to nano: recent advances in high-resolution microscopy, *Curr. Opin. Biotechnol.,* vol. 16, pp. 3–12, 2005.

[13] VisionGate Inc., Phoenix, AZ, USA. http://www.visiongate3d.com/.

[14] M. Fauver, E. J. Seibel, J. R. Rahn et al., Three-dimensional imaging of single isolated cell nuclei using optical projection tomography, *Opt Express,* vol. 13, pp. 4210–4223, 2005.

[15] N. Agarwal, A. M. Biancardi, F. W. Patten et al., Three-Dimensional DNA image cytometry by optical projection tomographic microscopy for early cancer diagnosis, *J. of Medical Imaging*, vol. 1(1), pp. 017501-017501, 2014.

[16] Flow Cytometry Facility, The Rabinovitch laboratory, http://www.pathology.washington.edu/research/labs/rabinovitch/flow room/protocols.php?p=1.

[17] P. S. Rabinovitch, DNA content histogram & cell-cycle analysis, *Methods Cell Biol*., vol. 41, pp. 263–296, 1994.

[18] A. Böcking, F. Giroud and A. Reith, Consensus report of the ESACP task force on standardization of diagnostic DNA image cytometry. European Society for Analytical Cellular Pathology, *Anal Cell Pathol.*, vol. 8, pp. 67-74, 1995.

[19] A. C. Kak and M. Slaney, Principles of Computerized Tomographic Imaging, *IEEE Press, New York*, 1988.

[20] Y. Boykov and G. Funka-Lea, Graph cuts & efficient N-D image segmentation, *Int. J. Computer Vision*, vol. 70, pp. 109-131, 2006.

[21] Y. Xie and A.P Reeves, Single 3D cell segmentation from optical CT microscope images. *Proc. Of SPIE Medical Imaging*, 2014.

[22] D. Zink, A.H. Fischer and J.A. Nickerson, Nuclear structure in cancer cells, *Nat Rev Cancer,* vol. 4, pp. 677-87, 2004.

[23] N. Johnson, M. Krebs, R. Boudreau et al., Actin-filled nuclear invaginations indicate degree of cell de-differentiation, *Differentiation*, vol. 71, pp. 414–424, 2003.

[24] P. S. Oud, A. G. Hanselaar, M. M. Pahlplatz et al., Image DNA-index (ploidy) analysis in cancer diagnosis, *Appl. Opt.,* vol. 26, pp. 3349–3355, 1987.

[25] F. Spyratos and M. Briffod, DNA ploidy & S-phase fraction by image & flow cytometry in breast cancer fine-needle cytopunctures, *Mod. Pathol.,* vol. 10, pp. 556–563, 1997.

[26] R. L. Coe and E. J. Seibel, Experimental & theoretical analysis for improved microscope design of Optical Projection Tomographic Microscopy, *Opt. Lett.,* vol. 38, pp. 3398-3401, 2013.

[27] D. A. Basiji, W. E. Ortyn, L. Liang et al., Cellular image analysis & imaging by flow cytometry, *Clinics in laboratory medicine,* vol. 27, pp. 653–670, 2007.

[28] K. Goda, A. Ayazi, D. R. Gossett et al., High-throughput single-microparticle imaging flow analyzer, *Proc. Natl. Acad. Sci.*, vol. 109, pp. 11630–11635, 2012.

[29] A. Nelson, M. Meyer, T. Neumann et al., Non-invasive Detection of Lung Cancer from Cells in Sputum Using Cell-CT™, presented at 15th World Conference of Lung Cancer, Sydney Australia, Oct 27-30, 2013.